Bulgarian Chemical Communications, Volume 51, Special Issue F (pp. 106 - 111) 2019

Numerical calculation of the permeability of fibrous porous medium

Zh.K. Akasheva[1,2*], B.K. Assilbekov[1,2], A.A. Kudaikulov[2]

[1] *Satbayev University, 22a Satbayev Str., Almaty, Kazakhstan, 050000*
[2] *LLP "KBTU BIGSoft", 140 Baitursynov Str., of.502, Almaty, Kazakhstan, 0500000*

Single-phase flow through a fibrous porous medium is numerically simulated. The simulation is based on the numerical solution of incompressible Navier-Stokes equations in irregular domains, where the irregular boundary is represented by its level-set function. This numerical method is used to search the Reynolds number below which the fluid flow in porous medium obeys linear Darcy's law for different kinds of porous medium. Also, the calculation results, which obtained using a simple and snap meshes, are compared with analytical solution. The results show that the simple mesh is effective enough and can be used instead of snap mesh in OpenFOAM.

Keywords: permeability, porous medium, mesh size, numerical calculation

[*] To whom all correspondence should be sent:
zhibek_akasheva@mail.ru

INTRODUCTION

Understanding of fluid flow mechanics through a porous medium is important in the design of many porous materials [1].

There are various approaches for fluid flow calculation in porous medium at pore-scale. In particular, pore network models [2-4] have been widely used to understand multiphase fluid displacement in porous media. Pore-network models are computationally efficient, and they are a viable tool for understanding multiphase flow at the pore scale. However, these methods are based on simplified geometries and physics, which limit their predictive capabilities [5].

Lattice Boltzmann model has been used to simulate flow through the true pore geometry of a porous media, for both single and multiphase flow. Lattice Boltzmann model is used to simulate two-fluid-phase flow at the pore scale [6]. However, the application of this model to multiphase flow is limited by the admissible range of fluid properties due to restricted numerical stability and its high computational cost.

Other approaches that use exact geometry as input to fluid flow numerical simulations in porous media include: volume of fluids [7, 8], smoothed particle hydrodynamics [9], level set [10], and density functional method [11]. Kudaikulov *et al*. predicted theoretically and numerically the permeability of an ordered fibrous porous medium for normal flows [12]. The theoretical prediction of velocity profile allows investigating in detail the fluid flow at the pore-scale or microscale.

In this work, numerical calculations are performed using the OpenFOAM finite volume library. Error analysis on the accuracy of numerical calculations is performed, and also, where possible, there is a comparison with the analytical solution.

MATHEMATICAL FORMULATION OF THE PROBLEM

This paper examines single-phase flow in fibrous porous media where porous material is represented as parallel periodic cylinders of equal radius (Fig.1a). Therefore, the domain with one cylinder in the middle can be considered. The flow direction is perpendicular to the axes of cylinders. Fig.1b shows boundary conditions used for this problem (*L* is the domain size).

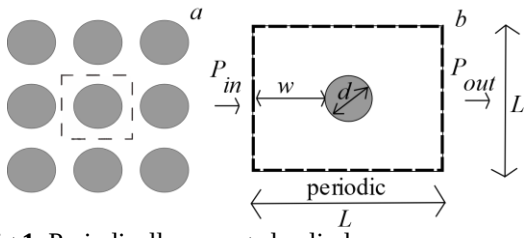

Fig.1. Periodically arranged cylinders

This model is based on numerical solution of the incompressible flow in irregular domains, where irregular boundary is represented by its level-set function [12]. The flow is described using the Navier-Stokes equations:

$$\frac{\partial \vec{u}}{\partial t} + \vec{u} \cdot \nabla \vec{u} = -\nabla P + \frac{1}{Re} \nabla^2 \vec{u} \quad (1)$$

$$\nabla \cdot \vec{u} = 0 \quad (2)$$

where u is the velocity, m/s; P is the pressure, Pa; and Re is the Reynolds number.

Initial condition for the velocity of fluid flow:

$$\vec{u}(0, x, y) = 0 \quad (3)$$

Boundary conditions on the boundaries of the domain (dashed lines on Fig.1b) are:

$$u(x = 0, y) = u(x = L, y) \quad (4)$$

$$u(x, y = 0) = u(x, y = L) \quad (5)$$

$$P(x = 0, y) = P_{in} \quad (6)$$

$$P(x = L, y) = P_{out} \quad (7)$$

$$P(x, y = 0) = P(x, y = L) \quad (8)$$

where P_{in} is the inlet pressure, Pa; P_{out} the outlet pressure, Pa.

No-slip boundary condition is used on the surface of the cylinders:

$$u(t, x, y)|_{d\Omega} = 0 \quad (9)$$

where $d\Omega$ is the surface of the cylinder.

SEARCHING OF REYNOLDS NUMBER FOR LINEAR DARCY'S LAW

Reynolds number below which the fluid flow in porous medium obeys linear Darcy's law in isotropic and anisotropic porous media is found in this section.

Whitaker examined that the linear Darcy's law is valid for Reynolds numbers Re<<1 using the method of volume averaging [13]. To investigate this condition, it is sufficient to calculate the permeability in linear Darcy's law, which is written as following for single-phase flow:

$$U = \frac{K}{\mu} \frac{P_{in} - P_{out}}{L} \quad (10)$$

where K is the absolute permeability, m^2; μ is the dynamic viscosity, Pa*s; and U the is volume-averaged velocity:

$$U = \frac{1}{V} \int_V u dV \quad (11)$$

where V is the volume, m^3.

In isotropic medium, all cylinders in the model are located at the same distance from each other and the coordinates of one cylinder are x_c=0.5 and y_c=0.5 and have a diameter of d=0.4. In anisotropic medium, cylinder C in the model is shifted relative to other cylinders (y_c has a different values) as shown in Fig.2. For this case, we move the location of the cylinder (y_c coordinate) and study the relation between the Reynolds number and permeability.

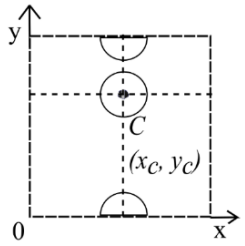

Fig.2. Anisotropic porous medium

Tabs.1-3 present the results of numerical calculation (υ^{-1} (inverse kinematic viscosity), U, Re and K (absolute permeability) for anisotropic porous medium for cylinders with d=0.2 and locations of middle cylinder y_c=0.5, 0.6 and 0.7, respectively.

Table 1. Calculation results for d=0.2 and y_c=0.5

υ^{-1}, $m^{-2}s$	U, ms^{-1}	Re	K, m^2
0.01	$1.57*10^{-4}$	$3.14*10^{-7}$	$1.57*10^{-2}$
0.1	$1.57*10^{-3}$	$3.14*10^{-5}$	$1.57*10^{-2}$
1	$1.57*10^{-2}$	$3.14*10^{-3}$	$1.57*10^{-2}$
10	$1.57*10^{-1}$	$3.13*10^{-1}$	$1.57*10^{-2}$
100	$8.36*10^{-1}$	$1.67*10^{0}$	$8.36*10^{-3}$

Table 2. Calculation results for d=0.2 and y_c=0.6

υ^{-1}, $m^{-2}s$	U, ms^{-1}	Re	K, m^2
0.01	$1.82*10^{-4}$	$3.63*10^{-7}$	$1.82*10^{-2}$
0.1	$1.82*10^{-3}$	$3.63*10^{-5}$	$1.82*10^{-2}$
1	$1.82*10^{-2}$	$3.63*10^{-3}$	$1.82*10^{-2}$
10	$1.81*10^{-1}$	$3.62*10^{-1}$	$1.81*10^{-2}$
100	$8.48*10^{-1}$	$1.70*10^{0}$	$8.48*10^{-3}$

Table 3. Calculation results for d=0.2 and y_c=0.7

υ^{-1}, $m^{-2}s$	U, ms^{-1}	Re	K, m^2
0.01	$2.57*10^{-4}$	$2.57*10^{-7}$	$2.57*10^{-2}$
0.1	$2.57*10^{-3}$	$2.57*10^{-5}$	$2.57*10^{-2}$
1	$2.57*10^{-2}$	$2.57*10^{-3}$	$2.57*10^{-2}$
10	$2.55*10^{-1}$	$2.55*10^{-1}$	$2.55*10^{-2}$
100	$8.54*10^{-1}$	$8.54*10^{0}$	$8.54*10^{-3}$

Fig.3 demonstrates the K-Re relationships for the anisotropic porous medium (cylinders with d=0.2 and locations of middle cylinder y_c=0.5, 0.6 and 0.7, respectively).

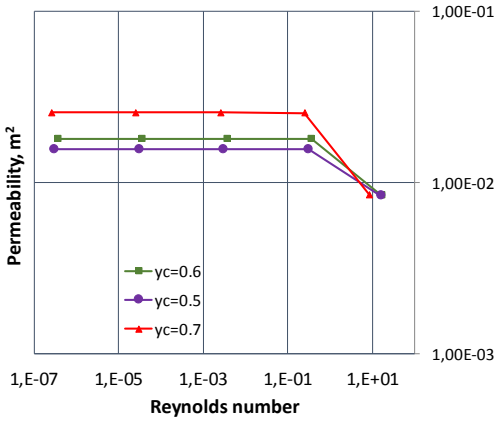

Fig.3. The K-Re for d=0.2 and y_c=0.5, 0.6 and 0.7, respectively

Fig.4 shows streamlines for the anisotropic porous medium (cylinders with d=0.2 and locations of middle cylinder y_c=0.5, 0.6 and 0.7, respectively) for kinematic viscosities 0.01 m^2/s and 0.1 m^2/s.

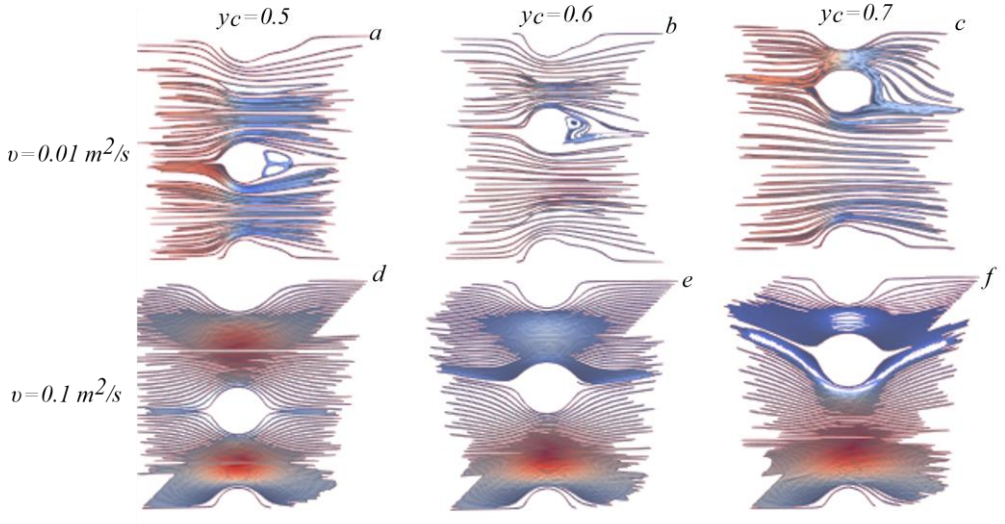

Fig.4. Streamlines for d=0.2 and y_c=0.5, 0.6 and 0.7 for υ=0.01 m^2/s and υ=0.1 m^2/s as indicated

From the numerical results, it can be seen that at lower values of Reynolds number, when vorticity does not occur, the linear Darcy's law is fulfilled. It is known that vorticity occurs at high values of Reynolds number [14] and appear inactive zones, therefore the permeability of porous medium depends not only on the geometry of porous medium, but also on the fluid flow properties (see Fig.4).

COMPARISON OF SIMPLE AND SNAP MESH

Results of numerical calculation using different computational meshes (simple and snap) are compared and affection of geometric inaccuracy on the results is studied in this section.

The simple structured mesh in the OpenFOAM is created using BlockMesh utility, which creates parametric meshes with grading and curved edges. The principle behind BlockMesh is to decompose the domain geometry into a set of 1 or more three dimensional, hexahedral blocks. Edges of the blocks can be straight lines, arcs or splines. Each block of the geometry is defined by 8 vertices, one at each corner of a hexahedron [15].

The snap mesh is created using SnappyHexMesh utility, which is a mesh generator that takes an already existing mesh (usually created with BlockMesh) and chisels it into the required mesh. SnappyHexMesh generates 3D meshes containing hexahedra and split-hexahedra automatically from triangulated surface geometries, or tri-surfaces. The mesh approximately conforms to the surface by iteratively refining a starting mesh and morphing the resulting split-hex mesh to the surface [16]. Fig.5a shows a simple mesh, Fig.5b shows a snap mesh in OpenFOAM.

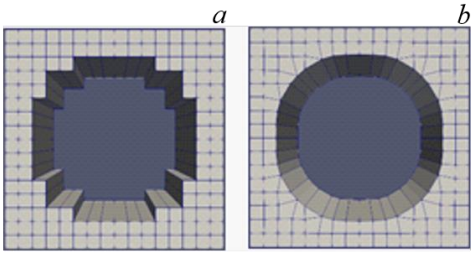

Fig.5. Simple (a) and snap (b) meshes

NUMERICAL RESULTS DISCUSSION

The optimal mesh size selection was studied in this section in order to achieve reliable calculation results while using the computational resources effectively. On one extreme, a rough mesh produces inaccurate results and on other hand, a too high-resolution mesh requires a large memory and high computational time. Therefore, mesh adaptation methods and an optimal choice of mesh resolution are necessary. Main parameters for optimal size selection are the diameter of cylinder *d* and parameter *w* (see Fig.1b).

$$w = \frac{L-d}{2} \qquad (12)$$

The accuracy of cylinder's surface depends on the mesh size. Therefore, the mesh resolution should be correlated with *d* and *w*. For our case the optimum mesh resolution was found by calculating the relative error of each mesh size relative *d* and *w*.

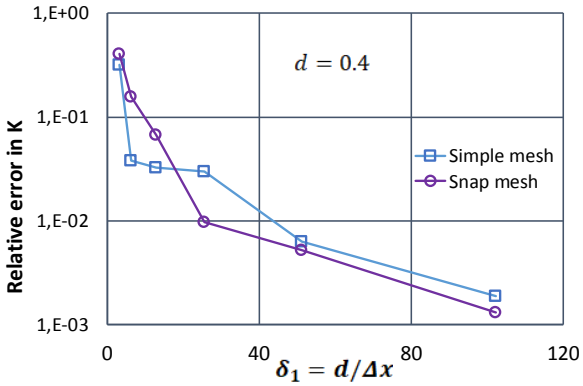

Fig.6. Relative error of average velocity for d=0.4 (simple and snap meshes)

The following formulas are used to calculate the relative errors of calculated permeability using simple and snap meshes:

$$RE = \frac{K_N - K_T}{K_T} \times 100\% \qquad (13)$$

$$RE_1 = \frac{K_{simple_{n*n}} - K_{simple_{512*512}}}{K_{simple_{512*512}}} \times 100\% \qquad (14)$$

$$RE_2 = \frac{K_{snap_{n*n}} - K_{snap_{512*512}}}{K_{snap_{512*512}}} \times 100\% \qquad (15)$$

where K_N is the numerical value of permeability, K_T is the theoretical value of permeability, K_{simple} is the permeability using simple mesh, K_{snap} is the permeability using snap mesh, *n* is the number of nodes along the x and y axes, respectively.

The calculation results for *d*=0.4 for simple and snap meshes are given on Fig.6 and Tab.4.

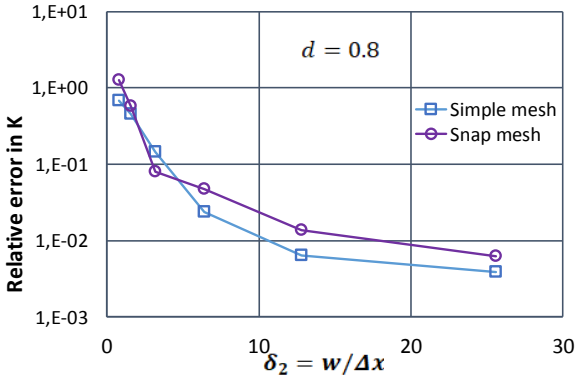

Fig.7. Relative error of average velocity for d=0.8 (simple and snap meshes)

The calculation results for d=0.8 for simple and snap meshes are given on Fig.7 and Tab.5.

Note that δ_1 is the ratio between the diameter of cylinder and mesh size ($\delta_1=d/\Delta x$) and δ_2 is the ratio between the parameter w and mesh size ($\delta_2=w/\Delta x$).

Table 4. Results for d=0.4 using simple and snap meshes

Mesh	δ_1	δ_2	K_{simple}, m^2	RE_1 of K_{simple}	K_{snap}, m^2	RE_2 of K_{snap}
8x8	6.4	0.8	$3.31*10^{-3}$	$6.78*10^{-1}$	$4.18*10^{-5}$	1.27
16x16	12.8	1.6	$2.65*10^{-3}$	$4.52*10^{-1}$	$2.90*10^{-5}$	$5.79*10^{-1}$
32x32	25.6	3.2	$1.56*10^{-3}$	$1.43*10^{-1}$	$1.98*10^{-5}$	$7.87*10^{-2}$
64x64	51.2	6.4	$1.78*10^{-3}$	$2.35*10^{-2}$	$1.92*10^{-5}$	$4.67*10^{-2}$
128x128	102.4	12.8	$1.84*10^{-3}$	$6.39*10^{-3}$	$1.86*10^{-5}$	$1.37*10^{-2}$
256x256	204.8	25.6	$1.83*10^{-3}$	$3.86*10^{-3}$	$1.85*10^{-5}$	$6.16*10^{-3}$
512x512	409.6	51.2	$1.82*10^{-3}$	0	$1.84*10^{-5}$	0

Table 5. Results for d=0.8 using simple and snap meshes

Mesh	δ_1	δ_2	K_{simple}, m^2	RE_1 of K_{simple}	K_{snap}, m^2	RE_2 of K_{snap}
8x8	3.2	2.4	2.29*10-2	3.18*10-1	4.71*10-2	4.04*10-1
16x16	6.4	4.8	3.48*10-2	3.82*10-2	3.88*10-2	1.56*10-1
32x32	12.8	9.6	3.47*10-2	3.27*10-2	3.58*10-2	6.71*10-2
64x64	25.6	19.2	3.26*10-2	2.95*10-2	3.39*10-2	9.59*10-3
128x128	51.2	38.4	3.33*10-2	6.25*10-3	3.37*10-2	5.18*10-3
256x256	102.4	76.8	3.35*10-2	1.86*10-3	3.36*10-2	1.30*10-3
512x512	204.8	153.6	3.36*10-2	0	3.36*10-2	0

COMPARISON OF NUMERICAL RESULTS WITH ANALYTICAL SOLUTION

The comparison of numerical results with analytical solution [17] is provided in this section.

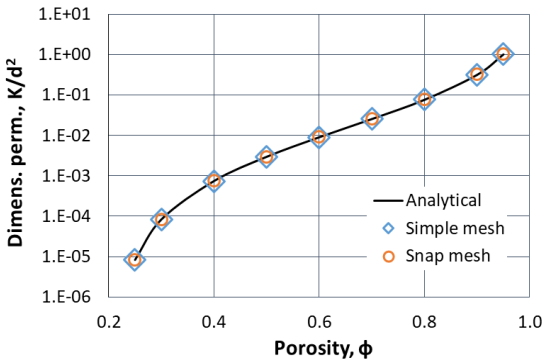

Fig.8. Comparison of numerical and analytical permeabilities

Tab.6 and Fig.8 present numerical results for simple and snap meshes for different radii of the cylinder (R), porosity (φ) and numerical predictions of dimensionless permeability using simple mesh (K_{simple}/R^2), snap mesh (K_{snap}/R^2) and dimensionless analytic permeability ($K_{analytic}/R^2$). Also, Tab.6 shows the comparison of relative errors of calculated permeability using simple and snap meshes, which are compared against the analytical values from [17].

It can be seen that the results are almost the same (relative error between the meshes is less than1%); therefore simple mesh can be used for calculation in OpenFOAM to save the computation time and power.

Table 6. Numerical results obtained using simple and snap meshes

Mesh	R, m	φ	K_{simple}/R^2	K_{snap}/R^2	$K_{analytic}/R^2$	RE of K_{simple}	RE of K_{snap}
128x128	0.1261	0.95	$1.02*10^{0}$	$1.31*10^{0}$	$1.01*10^{0}$	$1.17*10^{-2}$	$2.09*10^{-2}$
128x128	0.1784	0.90	$3.19*10^{-1}$	$3.23*10^{-1}$	$3.32*10^{-1}$	$7.34*10^{-3}$	$2.13*10^{-2}$
128x128	0.2523	0.80	$7.73*10^{-2}$	$7.79*10^{-2}$	$7.62*10^{-2}$	$1.42*10^{-2}$	$2.21*10^{-2}$
128x128	0.3090	0.70	$2.55*10^{-2}$	$2.60*10^{-2}$	$2.54*10^{-2}$	$2.69*10^{-3}$	$2.13*10^{-2}$
128x128	0.3568	0.60	$8.91*10^{-3}$	$9.15*10^{-3}$	$9.01*10^{-3}$	$1.13*10^{-2}$	$1.57*10^{-2}$
256x256	0.3989	0.50	$2.95*10^{-3}$	$2.98*10^{-3}$	$2.95*10^{-3}$	$1.14*10^{-3}$	$9.05*10^{-3}$
256x256	0.4370	0.40	$7.33*10^{-4}$	$7.51*10^{-4}$	$7.42*10^{-4}$	$1.32*10^{-2}$	$1.14*10^{-2}$
512x512	0.4720	0.30	$8.15*10^{-5}$	$8.43*10^{-5}$	$8.30*10^{-5}$	$1.77*10^{-2}$	$1.58*10^{-2}$
1024x1024	0.4886	0.25	$8.22*10^{-6}$	$8.40*10^{-5}$	$8.29*10^{-5}$	$8.45*10^{-3}$	$1.36*10^{-2}$

CONCLUSIONS

The permeability of fibrous porous medium is numerically calculated in this paper. The optimal mesh size is selected depending on the parameter *w* and the diameter of the cylinder *d*. The Reynolds number below which the flow obeys the linear Darcy's law is investigated for isotropic and anisotropic porous media.

The computational results show that the simple mesh is effective enough and can be used instead of snap mesh in OpenFOAM. From the Tab.6 it can be concluded that the correlation between the diameter of cylinder and mesh is effective enough for δ_1= 51.2 and δ_2=38.4 and can be applied for calculation of more complex porous medium. Numerical calculation results are in excellent agreement with analytical solution [17] for the flow in porous medium.

ACKNOWLEDGEMENTS

This work has been supported financially as part of the sub-project APP-JRG-17/0448F "Development and implementation of an integrated software product for a comprehensive solution of production stimulation problems on hydrocarbon fields" funded under the project "Stimulation of Productive Innovations". We thank PhD Ali Qaseminejad Raeini for his insightful comments on this work.

REFERENCES

[1] M.J. Blunt, Multiphase flow in permeable media. A pore-scale perspective. Cambridge Univ. Press, 2017.
[2] M.J. Blunt, P. King, *Transp. Porous Media*, **6**(4), 407 (1991).
[3] K. E. Thompson, *AIChE Journal* **48 (7),** 1369 (2002).
[4] M. Piri, M.J. Blunt, *Physical Review E* **71 (2),** (2005).
[5] M.J. Blunt, *Curr. Opin. Colloid Interface Sci.* **6 (3),** 197 (2001).
[6] C. Pan, M. Hilpert, C.T. Miller, *Water Resour. Res.* **40 (1),** (2004).
[7] A.Q. Raeini, M.J. Blunt, B. Bijeljicet, *J. Comput. Phys.*, **231**, 5653 (2012).
[8] H. Huang, P. Meakin, M.B. Liu, *Water Resour. Res.* **411 (12),** (2005).
[9] A.M. Tartakovsky, N. Trask, K. Pan, B. Jones, *Computat. Geosci.* **20 (4),** 1 (2015).
[10] M. Sussman, P. Smereka, S. Osher, *J. Comput. Phys.* **114 (1),** 146 (1994).
[11] O. Dinariev, N. Evseev, *Computat. Geosci.* **20 (4),** 1 (2015).
[12] A. Kudaikulov, C. Josserand, A. Kaltayev, Mathematical Modeling of Technological Processes, Series of Communications in Computer and Information Science, Book Series. - Springer **549**, **85** (2015).
[13] S. Whitaker, *Transp. Porous Media* 1, 3 (1986).
[14] G.K. Batchelor, An introduction to fluid dynamics, Cambridge Univ. Press, 2000.
[15] https://cfd.direct/openfoam/user-guide/v6-blockmesh/
[16] https://cfd.direct/openfoam/user-guide/v6-snappyhexmesh/
[17] A.S. Sangani, A.Acrivos, *Int.J.Multiphase flow*, **8**(3), 193 (1982).